Decays of the J/ψ into two pseudoscalar mesons

R. M. Baltrusaitis,[a] D. Coffman, J. Hauser, D. G. Hitlin, J. D. Richman,[b] J. J. Russell,[c] and R. H. Schindler
California Institute of Technology, Pasadena, California 91125

D. E. Dorfan,[d] F. Fabrizio,[d] F. Grancagnolo,[b] R. P. Hamilton,[e] C. A. Heusch, L. Köpke, R. Partridge,
J. Perrier, H. F. W. Sadrozinski, M. Scarlatella, T. L. Schalk, A. Seiden, and A. J. Weinstein
University of California at Santa Cruz, Santa Cruz, California 95064

J. J. Becker,[f] G. T. Blaylock, J. S. Brown, H. Cui,[g] B. I. Eisenstein, G. Gladding, S. A. Plaetzer,
A. L. Spadafora,[h] J. J. Thaler, A. Wattenberg, and W. J. Wisniewski
University of Illinois at Urbana-Champaign, Urbana, Illinois 61801

K. O. Bunnell, R. E. Cassell, D. H. Coward, K. F. Einsweiler,[b] L. Moss, R. F. Mozley, A. Odian,
J. R. Roehrig,[i] W. Toki, Y. Unno,[j] F. Villa, N. Wermes, and D. Wisinski
Stanford Linear Accelerator Center, Stanford, California 94305

T. H. Burnett, V. Cook, C. Del Papa,[b] A. L. Duncan, P. M. Mockett, A. Nappi,[k]
J. C. Sleeman,[l] and H. J. Willutzki
University of Washington, Seattle, Washington 98195
(Received 4 February 1985)

New results are obtained for the decays $J/\psi \to \pi^+\pi^-$ and $J/\psi \to K^+K^-$. The first observation of the decay $J/\psi \to K^0_S K^0_L$ is reported. Branching ratios are measured to be $(1.58 \pm 0.20 \pm 0.15) \times 10^{-4}$, $(2.39 \pm 0.24 \pm 0.22) \times 10^{-4}$, and $(1.01 \pm 0.16 \pm 0.09) \times 10^{-4}$, respectively. The corresponding electromagnetic form factors are $|F_{\pi^\pm}|^2 = (11.9 \pm 1.5 \pm 0.9) \times 10^{-3}$ and $|F_{K^\pm}|^2 = (20.9 \pm 2.1 \pm 1.5) \times 10^{-3}$. The K^0_S-K^0_L transition form factor $|F_{K^0_s \to K^0_L}|^2 = (8.9 \pm 1.4 \pm 0.5) \times 10^{-3}$ is obtained. A 90%-confidence-level upper limit of 5.2×10^{-6} is given for the branching ratio for the decay $J/\psi \to K^0_S K^0_S$. These form factors are substantially larger than expectations based on vector dominance and indicate large SU$_3$-symmetry-breaking effects.

I. INTRODUCTION

We report a high-statistics study of the J/ψ decays into two pseudoscalar mesons:

$$J/\psi \to \pi^+\pi^- \tag{1}$$

$$\to K^+K^- \tag{2}$$

$$\to K^0_S K^0_L \tag{3}$$

$$\to K^0_S K^0_S . \tag{4}$$

The G-parity-violating $\pi^+\pi^-$ mode and the SU$_3$-forbidden K^+K^- decay have been observed by previous experiments[1,2] with branching ratios of the order 10^{-4}. The suppression of these channels relative to direct J/ψ decays by a factor of 10 and the lack of observation of the $K^0_S K^0_L$ mode suggested[3] an electromagnetic origin for these decays and the SU$_3$-singlet nature of the J/ψ. To the extent that processes (1)–(3) proceed entirely through the electromagnetic interaction, their rates relative to $J/\psi \to \mu^+\mu^-$ directly measure the electromagnetic form factors of the pseudoscalar mesons. These form factors are of considerable importance as tests for models of mesonic wave functions used in QCD calculations.[4,5] In this paper we present measurements of branching ratios for processes (1)–(3), the electromagnetic form factors,

the scattering-angle distribution of reaction (3), and an upper limit on the decay (4).

II. THE APPARATUS

The Mark III detector,[6] located at SLAC's SPEAR storage ring, and its components have been fully described elsewhere.[7-13] We therefore summarize here only those elements relevant to this analysis. Figures 1(a) and 1(b) show cross sections of the spectrometer. Momenta of charged particles are measured in two cylindrical drift chambers placed in a solenoidal magnetic field of 4 kG, which cover a solid angle of $0.84 \times 4\pi$ sr and provide a momentum resolution of

$$\frac{\delta p}{p} = (0.015^2 + 0.015^2 p^2)^{1/2} , \tag{5}$$

where p is in GeV/c. The first term in (5) is due to multiple Coulomb scattering and the second is due to measurement errors in drift chambers. Charged-particle identification is obtained with a system of 48 time-of-flight (TOF) scintillation counters. These counters cover 80% of the solid angle and provide a time resolution of 190 ps for hadrons. This resolution allows a π/K separation of 1σ at a momentum of 1.5 GeV/c. Between the TOF counters and the coil of the solenoid is a gas-sampling
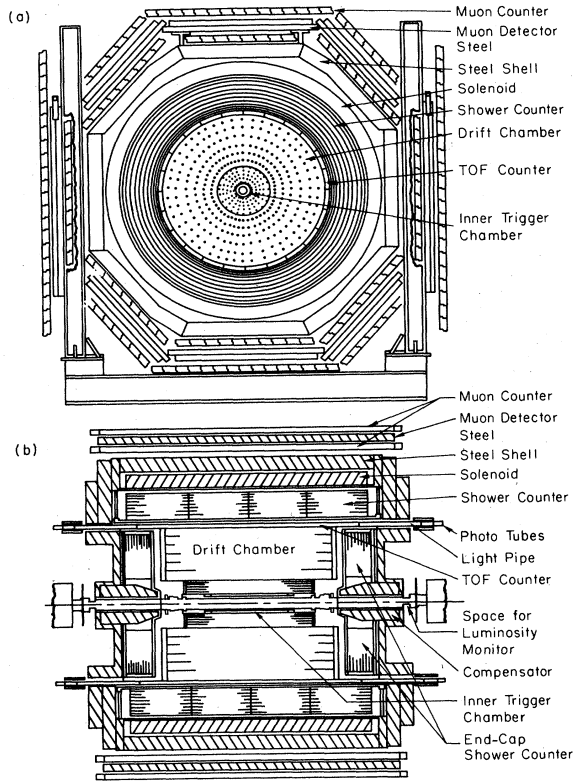
FIG. 1. A cross-sectional view of the Mark III detector, (a) transverse to beam axis, (b) parallel to beam axis.

electromagnetic calorimeter consisting of 24 layers of alternating 0.5-radiation-length lead sheets and proportional counters. The energy resolution $\delta E/E$ is $0.17/\sqrt{E}$, where E is the photon energy in GeV. This calorimeter, complemented by end-cap shower counters of similar design, covers 94% of the solid angle. The magnet is surrounded by two layers of proportional tubes separated by 13 cm of steel. This muon-detection system covers 65% of the solid angle. The data were taken with two trigger conditions. The first requires the existence of one track in the drift chamber in coincidence with a signal from a TOF counter. The second requires two tracks to be found in the drift chamber.

III. FLUX DETERMINATION

A. Total number of produced J/ψ's

The data sample was taken in two separate runs. One block, recorded just after completion of the detector, consists of 0.9×10^6 produced J/ψ's. The second set contains 1.8×10^6 J/ψ's. We describe the method used to evaluate the flux only for the second data set since the corresponding number for the first run is obtained by comparing the number of $\mu^+\mu^-$ pairs observed in the two runs (see Sec. III B below). Since the backgrounds from beam-gas interactions and cosmic rays as well as trigger efficiency and reconstruction systematics vary with the number of tracks, the data were first divided into one-prong, collinear two-prong, noncollinear two-prong, three-prong, and four-or-more-prong events. Four hundred one-prong, 2600 noncollinear two-prong and 1600 three-prong events and 1400 events with more than three prongs were then visually scanned to determine the backgrounds and systematics of the reconstruction program. The trigger efficiency is determined from a sample of $\sim10^5$ ψ' events. Using the decay mode $\psi'\rightarrow\pi^+\pi^-\psi$, the trigger efficiency is measured by tagging the two charged pions and then determining the trigger efficiency of the remainder of the event. For J/ψ decays with more than two prongs, the trigger efficiency is unity within the experimental uncertainty. For two-prong events it is $(95\pm1)\%$ and for one-prong events $(83\pm8)\%$. This method yields, in addition, the fraction of zero-prong J/ψ events (on which the Mark III detector does not trigger) to be $(3.5\pm0.5)\%$. The number of collinear two prongs is derived from the number of $\mu^+\mu^-$ pairs (see below) assuming that the branching ratios of $J/\psi\rightarrow\mu^+\mu^-$ and $J/\psi\rightarrow e^+e^-$ are equal. The results are summarized in Table I, where the errors are statistical only. Scaling the first-run sample with the number of $\mu^+\mu^-$ pairs yields a combined flux of $(2.71\pm0.06\pm0.15)\times10^6$ produced J/ψ's. The quoted systematic error corresponds to a 20% uncertainty for the background subtraction.

B. Total number of $\mu^+\mu^-$ pairs

The sample of $J/\psi\rightarrow\mu^+\mu^-$ is selected by requiring that events satisfy the following conditions:

TABLE I. Event classes and backgrounds of the second-run data only.

Class	Raw	Background	Population
>3 prongs	1 015 372	44 676±15 027	970 696±15 027
3 prongs	261 974	122 604±23 663	139 370±23 663
inelastic 2 prongs	586 400	245 702±40 049	363 098±40 122
elastic 2 prongs	206 976	1167±55	205 809±10 709
1 prong	92 306	53 537±8 490	46 910±8 490
0 prong	60 575±8 654		60 575±8 654
Σ			$(1.79\pm0.05)\times10^6$

(1) There are two and only two oppositely charged tracks.

(2) The acollinearity of the tracks is less than 3°.

(3) The momenta of the two tracks are between 1.408 and 1.676 GeV/*c*.

(4) At least three of the four muon layers have hits associated with these tracks.

(5) For both tracks $|\cos\theta_\mu|$ is less than 0.5 where θ_μ is the polar angle of the track. (This condition defines the acceptance of the muon detector for this analysis.)

(6) The time difference of the two tracks measured in the TOF system is less than 3 ns. (This eliminates cosmic-ray contamination.)

(7) Both tracks have measured shower energies in the barrel shower counter less than 0.735 GeV. (This reduces contamination by e^+e^- pairs.)

The acceptance is determined from Monte Carlo events to be $(39.8\pm0.7)\%$. The acceptance corrected number of $\mu^+\mu^-$ pairs then is $(152.8\pm1.6\pm5.1)\times10^3$. Radiative corrections have not yet been included. The angular distribution of the $\mu^+\mu^-$ pairs for part of the data is shown in Fig. 2 together with a fit of the form

$$dN/d\cos\theta_\mu \propto 1 + A\cos^2\theta_\mu \ .$$

The best fit is $A=1.03\pm0.05$, in agreement with expectations from QED and the quantum numbers of the J/ψ.

IV. ANALYSIS OF THE $J/\psi \rightarrow \pi^+\pi^-$ AND $J/\psi \rightarrow K^+K^-$ FINAL STATES

A. Event selection

The cuts applied to the raw data are required to reduce backgrounds from the leptonic decay modes $J/\psi \rightarrow e^+e^-$ and $J/\psi \rightarrow \mu^+\mu^-$ with branching ratios of 7% (Ref. 14) and to a lesser extent from the $J/\psi \rightarrow p\bar{p}$ decay, which occurs with a branching ratio of about 0.2% (Refs. 14 and 15). Other possible background sources are the three-body decays $J/\psi \rightarrow \rho^\pm\pi^\mp$ and $J/\psi \rightarrow K^\pm K^{*\mp}(892)$ with branching ratios of 1.0% and 0.34% (Refs. 14 and 16).
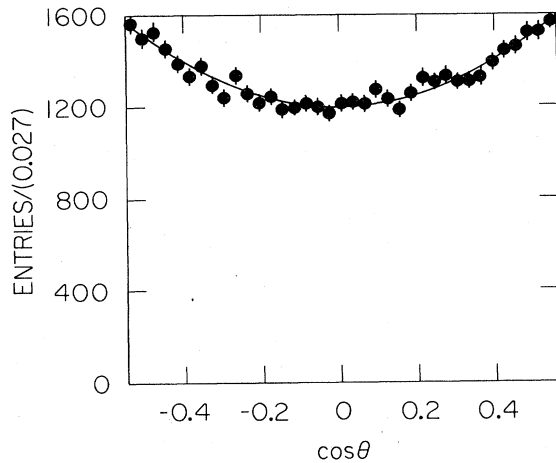
The accepted $\pi^+\pi^-$ and K^+K^- pairs are required to have the following characteristics:

(1) Two back-to-back (acollinearity less than 10°) oppositely charged tracks. This cut mainly removes contributions from $\rho\pi$ and $KK^*(892)$ final states.

(2) The normalized shower energy $E_{\text{norm}} = E_{\text{shower}} \times |\sin\theta|$ is less than 0.350 GeV for both tracks. This cut removes events of the type $J/\psi \rightarrow e^+e^-$ very efficiently (cf. quantitative discussion of backgrounds below).

(3) None or only one of the muon layers is hit.

(4) Each track has $|\cos\theta|$ less than 0.5.

(5) Each track has $|\cos\theta|$ greater than 0.04. This accounts for the dead space in the barrel shower counter at 90° where there is structural support for the lead sheets. Electron-positron pairs (called Bhabha pairs hereafter) in this region heavily contaminate the hadron pair sample.

(6) The measured momenta of both particles satisfy $1.34 \text{ GeV}/c < p < 1.75 \text{ GeV}/c$. The lower cut removes $J/\psi \rightarrow p\bar{p}$ events and the upper cut removes the remaining cosmic-ray background.

The surviving events are then subjected to a four-constraint (4C) kinematic fit to the hypotheses $J/\psi \rightarrow \pi^+\pi^-$, $J/\psi \rightarrow K^+K^-$, and $J/\psi \rightarrow p\bar{p}$. No events are found with a satisfactory χ^2 for the $p\bar{p}$ hypothesis. Figure 3 shows the scatter plot of the χ^2 for the remaining two possibilities $\pi^+\pi^-$ and K^+K^-. The hypothesis with the smaller χ^2 is chosen. Monte Carlo studies justify this procedure (see below). The lower χ^2 is also required to be less than 30. A check of the π-K separation is possible by calculating the square of the mass for each particle from the measured flight time and momentum. This is shown in Figs. 4(a) and 4(b). The peaks for the π and K sample are correctly centered at the appropriate masses. The separation of the two peaks is 1σ, corresponding to the measured resolution of the system.

Finally, the surviving 102 $\pi^+\pi^-$ candidates and 118 K^+K^- candidates are visually inspected to eliminate remaining e^+e^- and $\mu^+\mu^-$ pairs. 26 $\mu^+\mu^-$ events are
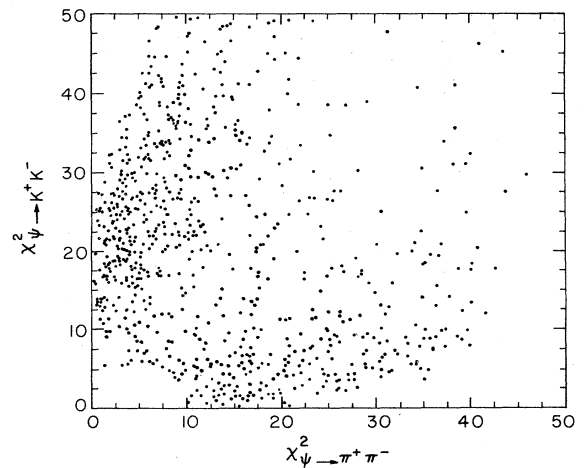

FIG. 2. Polar-angle distribution of $\mu^+\mu^-$ pairs.

FIG. 3. Scatter plot of the χ^2 for the $\pi^+\pi^-$ hypothesis versus the χ^2 of the K^+K^- hypothesis.
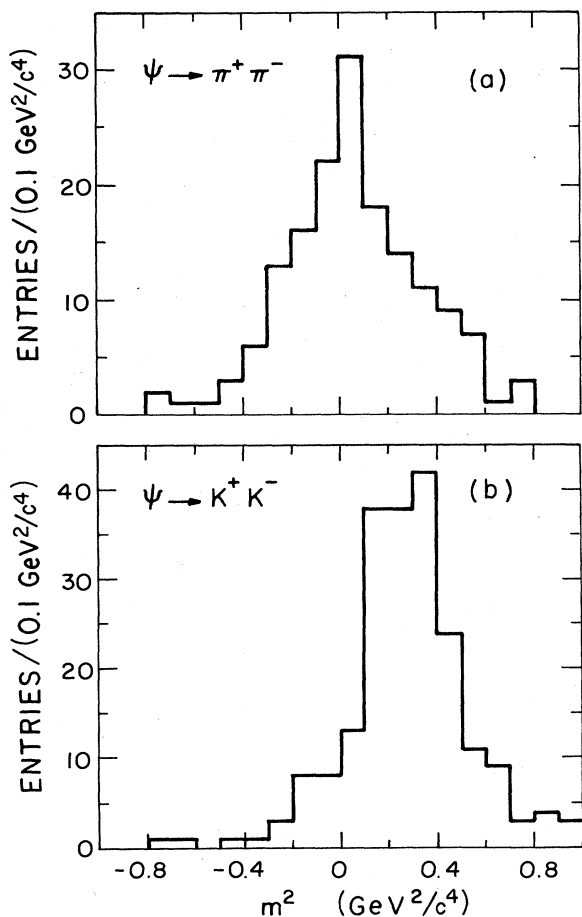
FIG. 4. TOF m^2 for (a) $\pi^+\pi^-$ events (b) K^+K^- events.

ed shower energy E_{norm} for the nontagged electron is shown in Fig. 5. The low-energy enhancement is attributed to spurious photons, events of the type $J/\psi\rightarrow\gamma e^+e^-$, and, of course, to some of the meson decays that are the subject of this paper. From this spectrum the measured probability for a single 1.55-GeV/c electron to deposit E_{norm} less than 0.350 GeV is smaller than $(2.8\pm0.3)\times10^{-3}$. With an estimated number of 90 000 Bhabha pairs (using less severe cuts than for tagging electrons), this yields a background of at most 0.7 events. This is an upper limit because we do not know how to separate the various contributions.

$\mu^+\mu^-$ pairs

High-energy pions and kaons can "punch through" and be detected in the muon system. On the other hand, high-energy muons might not be detected by the muon system. Inefficiency of the muon system can arise from hardware limitations and software reconstruction errors. The muon system measures the azimuth angle ϕ and the z coordinate for each hit. Hits must be associated with charged tracks within 3σ of the expected coordinates to be accepted as muon candidates. Because the $\mu^+\mu^-$ rate is so large compared with the two-body hadronic modes of the J/ψ, a small inefficiency of the muon-detection system can result in a large leakage into the dihadron signal.

To estimate muon contamination of the $\pi^+\pi^-$ data sample, the individual probabilities for a muon to hit either zero or one muon layer are measured as follows. Muon events are tagged as high-momentum collinear events with one track having a hit in both muon layers. The other track is then used to determine the probability for a muon to hit zero or one layer. Muon hits are deter-
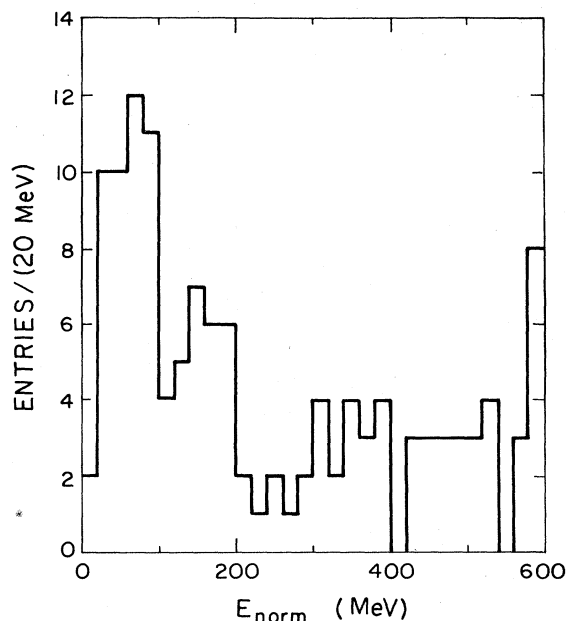
eliminated by this scan because of misassociated tracks in the muon system. This number agrees with expectations from multiple Coulomb scattering in the detector. After removing these events our final sample consists of 84 $\pi^+\pi^-$ and 110 K^+K^- events.

B. Background estimation

Since the momentum difference between leptons and pions in the decays $J/\psi\rightarrow$leptons and $J/\psi\rightarrow\pi^+\pi^-$ is less than 0.006 GeV/c, momentum measurements alone cannot be used to distinguish muons or Bhabha pairs from pions.

e^+e^- pairs

The e^+e^- contamination of the pion signal is estimated by measuring the shower energy for Bhabha pairs. Bhabha pairs are tagged by requiring that the modulus of the vector sum of the two charged particle momenta is less than 0.1 GeV/c. In addition, one track is required to deposit more than 1.2 GeV into the shower counter and both tracks must satisfy the same solid-angle cuts that are applied to the $J/\psi\rightarrow\pi^+\pi^-$ and $J/\psi\rightarrow K^+K^-$ signals. This results in a sample of 33 800 tagged electrons. The low-energy end of the spectrum of the normalized deposit-

FIG. 5. Normalized deposited shower energy for unbiased e^+e^- pairs.

mined by visually scanning event pictures. This procedure yields a probability of 3×10^{-2} per track for one layer to be hit, and a probability of 4×10^{-4} per track for no layer to be hit. With 60 000 $\mu^+\mu^-$ events in the relevant solid angle this leads to an estimated background of 1.4 muon pairs in the $\pi^+\pi^-$ sample.

$\rho^{\pm}\pi^{\mp}$ and $K^{\pm}K^{*\mp}$ (892) final states

The possible contribution of these events is estimated using a Monte Carlo simulation. On the basis of no events found to simulate the $\pi^+\pi^-$ or K^+K^- final state an upper limit of four events for the $\pi^+\pi^-$ case and 2.5 events for the K^+K^- case can be placed at a 90% confidence level.

C. Acceptance calculation

Solid angle and reconstruction efficiency. The acceptance is determined from a Monte Carlo simulation. This simulation includes $\pi^{\pm} \to \mu^{\pm}\nu$ and $K^{\pm} \to \mu^{\pm}\nu$ decays and the 4C fit procedure described earlier. The results are 0.622 ± 0.017 for the $\pi^+\pi^-$ final state and 0.502 ± 0.016 for the K^+K^- case, assuming a $\sin^2\theta$ distribution.

Hadronic signature. The acceptance of the cuts for a hadronic signature in the shower counter is measured using the high-momentum pion from the decay channel $J/\psi \to \rho^{\pm}\pi^{\mp}$ and the high-momentum kaon from the decay channel $J/\psi \to K^{\pm}K^{*\mp}$(892). The results are 0.391 ± 0.008 for $\pi^+\pi^-$ and 0.434 ± 0.019 for K^+K^-. This acceptance does not include the solid angle.

Hadronic punchthrough. An estimate of hadronic punchthrough is made as follows: First, punchthrough, as determined with the off-line reconstruction program, is estimated using high-momentum pions and kaons from the decays $J/\psi \to \rho^{\pm}\pi^{\mp}$ and $J/\psi \to K^{\pm}K^{*\mp}$(892). The cuts used to isolate these events are described elsewhere.[16] The punchthrough probabilities for pions and kaons based on this analysis are 0.172 ± 0.002 and 0.225 ± 0.006, respectively.

Second, the loss of signal resulting from the visual inspection is estimated with a scan of about 100 events of each of the modes $J/\psi \to \rho^{\pm}\pi^{\mp}$, $K^{\pm}K^{*\mp}$(892). The result of this scan is a loss of $(9.9 \pm 0.3)\%$ of the pions and $(2.3 \pm 0.02)\%$ of the kaons.

Combining all these results from the previous discussion finally yields an acceptance of (0.181 ± 0.009) for the $\pi^+\pi^-$, and (0.165 ± 0.010) for the K^+K^- final state.

D. Radiative corrections for $J/\psi \to \mu^+\mu^-$, $\pi^+\pi^-$, and K^+K^-

Radiative corrections must be calculated for the case of radiation from the final state only. Because we are interested only in ratios of branching ratios, corrections for radiation from the initial state cancel due to the small width of the J/ψ. The corrections are calculated according to[17]

$$\sigma = \sigma_0 t \int_0^{k_{max}} \frac{dk}{2k} \left[\frac{k}{E} \right]^t \left[1 + \left[1 - \frac{k}{E} \right]^2 \right], \quad (6)$$

where σ_0 is the zeroth-order cross section,

$$t = \frac{2\alpha}{\pi} \left[\ln \frac{4E^2}{m^2} - 1 \right]$$

(α is the fine-structure constant), $m = m_{\mu\pm}$, $m_{\pi\pm}$, or $m_{K\pm}$, E is the beam energy, k is the energy of the radiated photon, and k_{max} is the maximum possible unobserved photon energy. The quantity k_{max} is slightly different (0.261 GeV for $\mu^+\mu^-$, 0.141 GeV for $\pi^+\pi^-$, and 0.196 GeV for K^+K^-) for the three reactions due to the different particle masses and different procedures used to identify the final states. Formula (6) yields corrections of -5.0% for the $\mu^+\mu^-$, -5.8% for the $\pi^+\pi^-$, and -2.7% for the K^+K^- final state.

V. ANALYSIS OF THE $J/\psi \to K_S^0 K_L^0$ FINAL STATE

A. Event selection

The decay $J/\psi \to K_S^0 K_L^0$ is identified by the reconstruction of the decay $K_S^0 \to \pi^+\pi^-$ with the correct K_S^0 momentum of 1.468 GeV/c. The main backgrounds are the decays $J/\psi \to \rho^0\pi^0$ where the ρ has a recoil momentum of 1.449 GeV/c, and $J/\psi \to K_S^0 K^{*0}$(892)$\to K_S^0 K_L^0 \pi^0$ where the K_S^0 has a recoil momentum of 1.373 GeV/c. The branching ratios of these two processes are large compared to the $K_S^0 K_L^0$ signal; stringent cuts therefore must be applied to isolate the signal. Other contributing backgrounds are any decays of the form $J/\psi \to \pi^+\pi^-$ + photons. These backgrounds are distinguishable from $J/\psi \to K_S^0 K_L^0$ when two or more photon tracks in the shower counter are detected.

Figure 6 provides an illustration of the relevant geometrical information used for shower-counter tracks. For this analysis, two quantities are determined using shower-counter information. The first is the number of photons N_γ. Interacting charged tracks can generate nearby hits

EVENT 7228, RUN 1470
TRACK LIST

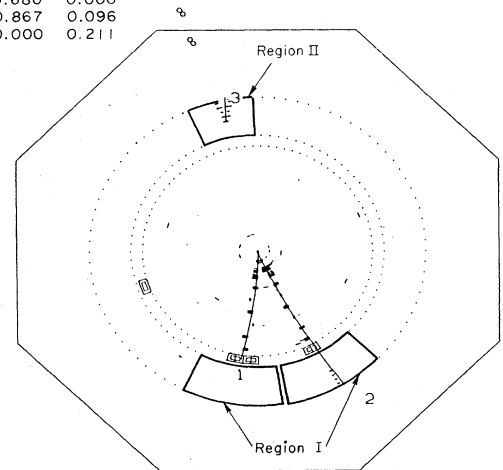| N	P(GeV/c)	E(GeV)
1	0.680	0.000
2	0.867	0.096
3	0.000	0.211

FIG. 6. Example of a $J/\psi \to K_S^0 K_L^0$ event with interacting K_L^0. (For reasons of clarity the regions I and II are not to scale).

which can be misinterpreted as photons. Therefore, a region (I) is defined where photons are not counted. Region I (see Fig. 6) is a cone of half-angle δ centered on charged tracks where $\cos\delta=0.95$.

The second quantity (M) is the invariant mass of that pair out of all possible photon pairs which is closest to the mass of the π^0. Since an interacting K_L^0 produces hits which can be misidentified as photons, a second region (II) is defined. It is a cone centered on the missing momentum with half-angle ϵ and $\cos\epsilon=0.995$. Photons in this region are not included in the calculation of M. However, they are included in the quantity N_γ.

Selected events satisfy the following criteria:

(1) There are two and only two oppositely charged tracks.

(2) The invariant mass for the pair is in the range $0.470 < m_{\pi\pi} < 0.520$ GeV/c^2, assuming each charged track is a pion.

(3) Charged tracks form a secondary vertex separated from the beam axis by more than 9 mm in the xy projection perpendicular to the beam. The distribution of the distance R_{xy} of the secondary vertex from the beam is shown in Fig. 7 for events satisfying criterion 1. We have checked our vertex finding efficiency by measuring the K_S^0 lifetime from the mode $J/\psi\to K_S^0 K^{*0}(892)$. Figure 8 shows a comparison of data and Monte Carlo events.

(4) The mass M is outside the interval $0.11 < M < 0.17$ GeV/c^2.

B. Signal determination

Figure 9 shows the resulting K_S^0 momentum spectrum after cuts. The effect of requiring progressively fewer photons is shown in histograms (a) through (f). There is a peak at a momentum of 1.47 GeV/c for all N_γ and another more rapidly decreasing peak at 1.37 GeV/c that finally vanishes when $N_\gamma=0$. The high-momentum peak arises from $J/\psi\to K_S^0 K_L^0$ while the lower one is due to $J/\psi\to K_S^0 K^{*0}(892)$.
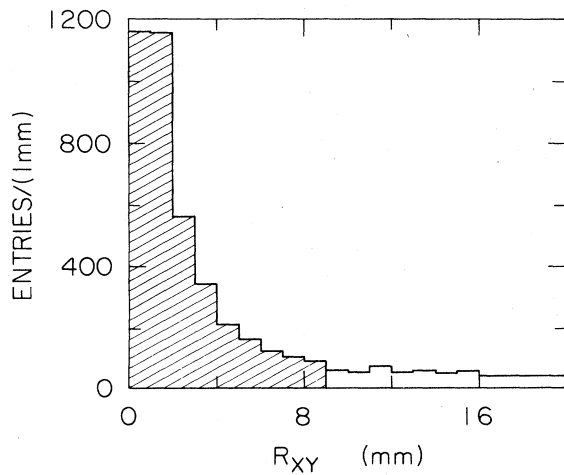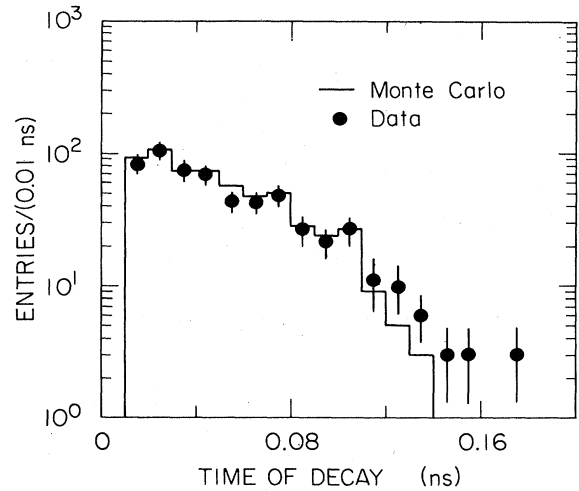
FIG. 8. K_S^0 decay time for data and Monte Carlo events from the mode $J/\psi\to K_S^0 K^{*0}(892)$.

We want to obtain the largest unbiased sample of $K_S^0 K_L^0$ events possible. In order to study the backgrounds for each N_γ, a maximum likelihood fit is made with the hypothesis of two Breit-Wigner shaped peaks folded with the resolution plus a quadratic background. The $KK^*(892)$ momentum peak is fixed at 1.373 GeV/c and the momentum width of the $K^*(892)$ at 0.016 GeV/c. The position and the area of the $K_S^0 K_L^0$ peak is determined by the fit, with its intrinsic momentum width fixed at zero. The σ for the $KK^*(892)$ peak is fixed at 0.020 GeV/c. In the $K_S^0 K_L^0$ region the momentum resolution is determined by the fit. From Table II one sees that the fixed momentum resolution agrees with the fitted σ of the $K_S^0 K_L^0$ peak. For $N_\gamma\le 4$, the angular distribution of the K_S^0 in the signal region is shown together with a Monte Carlo simulation for a $\sin^2\theta_{K_S^0}$ distribution (see Fig. 10).
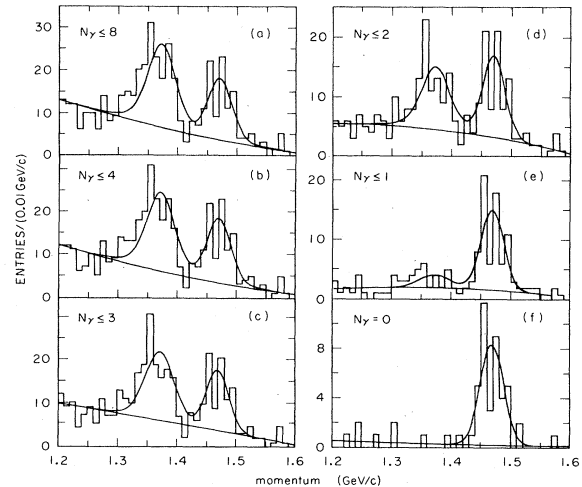
FIG. 7. Transverse distance of vertex from beam line. The shaded area contains excluded events.

FIG. 9. K_S^0 momentum spectrum as a function of the N_γ cut.

TABLE II. $J/\psi \to K_S^0 K_L^0$ signal and background summary.

N_γ	Number of KK^* Events	Number of $K_S K_L$ events	$K_S K_L$ Mean momentum (GeV/c)	$K_S K_L$ sigma momentum (GeV/c)
≤ 8	129 ± 16	71.7 ± 10.3	1.472 ± 0.003	0.020 ± 0.003
≤ 4	124 ± 14	73.7 ± 11.0	1.472 ± 0.003	0.020 ± 0.003
≤ 3	107 ± 17	65.1 ± 13.0	1.471 ± 0.003	0.019 ± 0.003
≤ 2	68 ± 15	61.1 ± 12.0	1.470 ± 0.003	0.018 ± 0.003
≤ 1	15 ± 9	64.3 ± 8.4	1.469 ± 0.003	0.019 ± 0.002
0	0 ± 5	39.4 ± 8.4	1.468 ± 0.003	0.019 ± 0.003

$N_\gamma \leq 4$ is chosen for the calculation of the branching ratio. Note that the $K_S^0 K_L^0$ signal for $N_\gamma = 0$ is significantly lower than that for $N_\gamma = 1$. This is a result of K_L^0 interactions which produce a photon signal in region II. The probability that a K_L^0 will produce a detectable signal in the shower counter, estimated from a sample of identified K_L^0 in the decay sequence

$$J/\psi \to K_L^0 K^{*0}(892) ,$$
$$\qquad \quad \big\downarrow K^\pm \pi^\mp$$

is found to be about 50%. This is in reasonable agreement with the observed decrease in the $K_L^0 K_S^0$ signal in the distribution with $N_\gamma = 0$.

The acceptance for the decay $J/\psi \to K_S^0 K_L^0$ is determined using the Monte Carlo procedure to be 0.269 ± 0.010. This simulation does not include criterion 4.

VI. ANALYSIS OF THE $K_S^0 K_S^0$ FINAL STATE

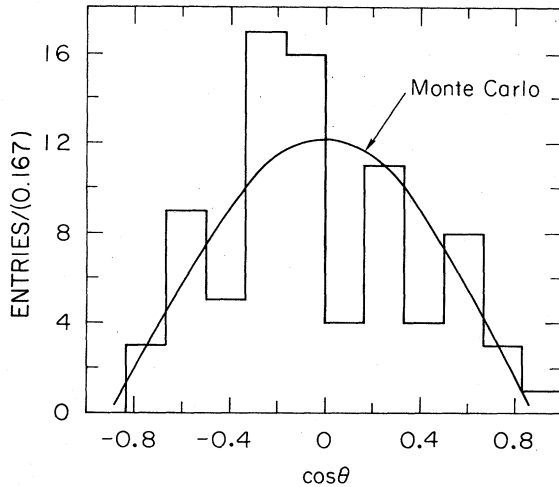Candidates for this decay satisfy the following conditions:

(1) There are four and only four charged tracks with net charge zero.

(2) There are two and only two neutral effective mass combinations per event with $0.47 < M_{\pi^+ \pi^-} < 0.52$ GeV/c^2 assuming the particles to be pions.

(3) There are two detached vertices with $R_{xy} > 9$ mm each.

(4) The remaining events are then subjected to a 4C fit to the hypothesis $J/\psi \to K_S^0 K_S^0$. Figure 11 shows the resulting $K_S^0 K_S^0$ invariant mass spectrum for events with a χ^2 less than 30.0. There are no events with $m_{K_S^0 K_S^0}$ greater than 3.00 GeV/c^2. The acceptance $\epsilon = 0.165 \pm 0.02$ is calculated with Monte Carlo events generated with a flat angular distribution.

VII. SUMMARY OF RESULTS AND DISCUSSION

We summarize the results on the four pseudoscalar-pseudoscalar channels in Table III. The results are given both as branching ratios and electromagnetic form factors $|F_h|$, defined by[18]

$$\sigma(e^+ e^- \to h^+ h^-) = \sigma(e^+ e^- \to \mu^+ \mu^-)\frac{\beta_h^3}{4}|F_h|^2 , \qquad (7)$$

FIG. 10. Angular distribution for K_S^0's for 1.44 GeV/$c < p_{K_S^0} < 1.54$ GeV/c. The solid curve shows the Monte Carlo curve for a $\sin^2\theta$ distribution.
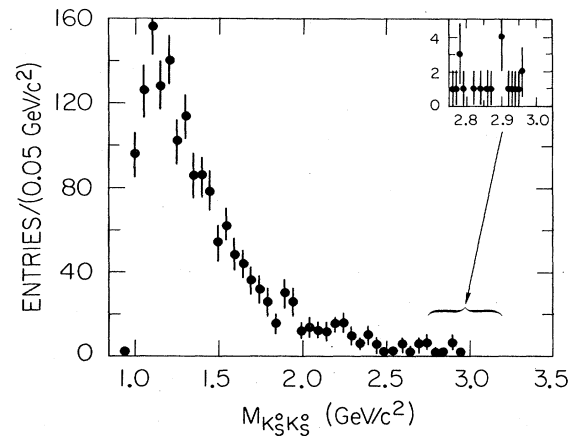

FIG. 11. Invariant $K_S^0 K_S^0$ mass spectrum in 0.05 GeV/c^2 bins. The inset shows the upper end of the same spectrum in 0.01 GeV/c^2 bins.

TABLE III. Event numbers, branching ratios, and form factors.

Final state	Events	Corr. events	Acceptance	$10^4 B \left[\dfrac{J/\psi \to h\bar{h}}{J/\psi \to \text{all}} \right]$	$10^3 \| F_h \|^2$
$J/\psi \to \pi^+\pi^-$	84	77.8	0.181	$1.58 \pm 0.20 \pm 0.15$	$11.85 \pm 1.50 \pm 0.91$
$\to K^+K^-$	110	107.0	0.165	$2.39 \pm 0.24 \pm 0.22$	$20.94 \pm 2.10 \pm 1.54$
$\to K_S^0 K_L^0$	73.7	73.7	0.269	$1.01 \pm 0.16 \pm 0.09$	$8.9 \pm 1.4 \pm 0.5$
$\to K_S^0 K_S^0$	<2.3	<2.3	0.165	<0.052	

where β_h is the velocity of the hadron. Our results are in quantitative agreement with previous experiments for the $\pi^+\pi^-$ and K^+K^- final states.[1,2] Assuming these decays are electromagnetic (for a discussion of gluon contributions see Ref. 19) we compare our measured form factors with a simple pole model inspired by vector dominance,[20]

$$F_{\pi^\pm} = \frac{m_\rho^2}{\Delta_\rho},$$

$$F_{K^\pm} = \frac{1}{2}\frac{m_\rho^2}{\Delta_\rho} + \frac{1}{6}\frac{m_\omega^2}{\Delta_\omega} + \frac{1}{3}\frac{m_\phi^2}{\Delta_\phi}, \qquad (8)$$

$$F_{K^0} = -\frac{1}{2}\frac{m_\rho^2}{\Delta_\rho} + \frac{1}{6}\frac{m_\omega^2}{\Delta_\omega} + \frac{1}{3}\frac{m_\phi^2}{\Delta_\phi},$$

where $\Delta_i \equiv s - m_i^2$, thus neglecting the small imaginary part of the form factor far away from the pole.

Evaluation of (8) gives $|F_{\pi^\pm}|^2 = 4.3 \times 10^{-3}$, $|F_{K^\pm}|^2 = 7.2 \times 10^{-3}$, and $|F_{K^0}|^2 = 0.36 \times 10^{-3}$, in clear contradiction to our measurements (see Table III). Our results are consistent with the results from the Orsay[21] and Novosibirsk groups[20,22] in the 1–2-GeV c.m.s.-energy region which indicate the existence of higher-mass vector mesons, thus giving a larger form factor at the J/ψ mass.

In first-order QCD calculations[4,5] the meson form factors are given by a series expansion whose leading term is related to the pion (kaon) decay constant $f_{\pi(K)}$ by

$$F_{\pi(K)}(Q^2) \underset{Q^2 \to \infty}{=} 16\pi \alpha_s(Q^2) \frac{(f_{\pi(K)})^2}{Q^2}. \qquad (9)$$

Taking Eq. (9) at face value requires $\alpha_s(Q^2) \sim 2$ to explain the magnitude of the measured form factors (with $f_\pi = 0.093$ GeV and $f_K = 0.113$ GeV). It is therefore not adequate at our Q^2 to use just the leading term of the first-order expansion. Since the relevant value of Q^2 in Eq. (9) is not obvious,[23] we form the ratio $(F_K/F_\pi)^2 = (f_k^2/f_\pi^2)^2 = 2.18$ from Eq. (9), in which Q^2 is not an explicit variable. This number is compatible with

our measured value of $1.77 \pm 0.29 \pm 0.15$. This result for the ratio is free of flux uncertainties and most of the possible systematic errors. However, the derivation[24] of Eq. (9) assumes only even terms in the mesonic wave functions. This assumption also implies a vanishing rate for $J/\psi \to K_S^0 K_L^0$ which we observe with a sizable branching ratio.[25] Our data thus indicate that the neglected odd components are important for the kaon wave function. This may not be too surprising since the masses of the strange quark and the up and down quarks are quite different.

In another approach[26] based on mixing of the J/ψ with vector mesons, predictions have been made for the three modes investigated in this experiment. From this model branching ratios of 1.2×10^{-4} for the $\pi^+\pi^-$, 2.7×10^{-4} for the K^+K^-, and 0.4×10^{-4} for the $K_S^0 K_L^0$ final state are predicted. There is reasonable agreement with the data for the $\pi^+\pi^-$ and K^+K^- cases, whereas the calculation falls short for the $K_S^0 K_L^0$ channel by a factor of 2.5.

Finally, an upper limit of 5.2×10^{-6} is given on the decay $J/\psi \to K_S^0 K_S^0$, a reaction forbidden by the spin-statistics theorem. It has been suggested[27] that a mechanism related to the Einstein-Podolsky-Rosen hypothesis[28] could lead to $K_S^0 K_S^0$ events at a rate of a few times 10^{-8}. The sensitivity of our experiment is not sufficient to probe this regime of branching ratios.

VIII. ACKNOWLEDGMENTS

[a]Present address: Physics Dept., Univ. of Utah, Salt Lake City, UT 84112.
[b]Present address: CERN, EP, 1211 Geneva 23, Switzerland.
[c]Present address: International Imaging Systems, Milpitas, CA 95035.
[d]Present address: Applied Technology, Sunnyvale, CA 94086.
[e]Present address: Anadrill/Schlumberger, Sugarland, TX 77478.
[f]Present address: ESL, Sunnyvale, CA 94088-3510.
[g]Present address: Institute of High Energy Physics, Beijing, China.
[h]Present address: ORSAY, LAL, France.

[i]Present address: Lockheed Research, Palo Alto, CA 94302.

[j]Present address: Phys. Dept., KEK Tsukuba, Ibaraki 305, Japan.

[k]On leave of absence from Univ. of Pisa, Pisa, Italy.

[l]Present address: Physics Dept., Northeastern Univ., Boston, MA 02115.

[1]W. Braunschweig *et al.*, Phys. Lett. **63B**, 487 (1976). R. Brandelik *et al.*, Z. Phys. C **1**, 233 (1979).

[2]F. Vanucci *et al.*, Phys. Rev. D **15**, 1814 (1977).

[3]F. J. Gilman, in *High Energy Physics and Nuclear Structure—1975*, proceedings of the Sixth International Conference, Santa Fe and Los Alamos, edited by D. E. Nagle, R. L. Burman, B. G. Storms, A. S. Goldhaber, and C. K. Hargrave (AIP, New York, 1975), p. 331.

[4]G. B. Lepage *et al.*, in *Particles and Fields—2*, proceedings of the Banff Summer Institute, Banff, Canada, 1981, edited by A. Z. Capri and A. N. Kamal (Plenum, New York, 1983), p. 83, and literature quoted therein.

[5]S. J. Brodsky *et al.*, in *Particles and Fields—2* (Ref. 4), p. 143, and literature quoted therein.

[6]D. Bernstein *et al.*, Nucl. Instrum. Methods **226**, 301 (1984).

[7]J. Roehrig *et al.*, Nucl. Instrum. Methods **226**, 319 (1984).

[8]J. S. Brown *et al.*, Nucl. Instrum. Methods **221**, 503 (1984).

[9]W. Toki *et al.*, Nucl. Instrum. Methods **219**, 479 (1984).

[10]R. Fabrizio *et al.*, Nucl. Instrum. Methods **227**, 220 (1984).

[11]J. J. Thaler *et al.*, IEEE Trans. Nucl. Sci. NS-30, 236 (1982).

[12]A. L. Spadafora, Ph.D. thesis, University of Illinois, 1984.

[13]J. J. Becker, Ph.D. thesis, University of Illinois, 1984.

[14]Particle Data Group, Phys. Lett. **111B**, 1 (1982).

[15]J. S. Brown, Ph.D. thesis, University of Washington, 1984.

[16]K. F. Einsweiler, Ph.D. thesis, Stanford University, 1984.

[17]H. D. Schulz, Report No. DESY F39-70/1, 1970 (unpublished); and private communications from Y. S. Tsai.

[18]M. L. Perl, *High Energy Physics* (Wiley, New York, 1974), p. 499.

[19]S. Nussinov and M. G. Olsson, Durham Report No. DTP/84/18, 1984 (unpublished).

[20]P. M. Ivanov *et al.*, Phys. Lett. **107B**, 297 (1981).

[21]F. Mané *et al.*, Phys. Lett. **99B**, 261 (1981).

[22]A. D. Bukin *et al.*, Phys. Lett. **73B**, 226 (1978).

[23]S. J. Brodsky, G. P. Lepage, and P. B. Mackenzie, Phys. Rev. D **28**, 228 (1983).

[24]S. J. Brodsky and G. P. Lepage, Phys. Rev. D **22**, 2157 (1980).

[25]Previously only an upper limit of 8.9×10^{-5} was available (see Ref. 2).

[26]L. J. Clavelli and G. W. Intemann, Phys. Rev. D **28**, 2767 (1983).

[27]M. Roos, Helsinki Report No. HU-TFT-80-5, 1980 (unpublished).

[28]A. Einstein, B. Podolsky, and N. Rosen, Phys. Rev. **47**, 777 (1935).